Photochemical reactions between dinuclear metal carbonyl complexes and alkyl halides. Formal oxidative addition across a metal–metal single bond proceeding by a free radical chain mechanism

**Michael A. Biddulph, Reg Davis * and Fiona I.C. Wilson**

School of Applied Chemistry, Kingston Polytechnic, Penrhyn Road, Kingston upon Thames, KT1 2EE (U.K.)
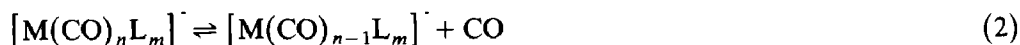
(Received November 24th, 1989)

Abstract

Photochemical reactions between $[Mn_2(CO)_8L_2]$ (L = CO, PBu_3, PEt_3, $P(OMe)_3$, $P(OPh)_3$, PPh_3) and alkyl halides (RX) yield both alkyl and halo complexes, $[MnR(CO)_4L]$ and $[MnX(CO)_4L]$, in equimolar quantities. Kinetic and quantum yield studies suggest that these reactions proceed by a radical chain pathway involving CO dissociation from the dinuclear complex and metal–metal bond homolysis of the coordinatively unsaturated dinuclear intermediate.

Introduction

There has been considerable interest in photochemical reactions of metal–metal bonded dimers of the type $[L_m(OC)_nM-M(CO)_nL_m]$. Many of these processes proceed by metal–metal bond homolysis (eq. 1) and thus, in these cases, the

$$[L_m(OC)_nM-M(CO)_nL_m] \rightleftharpoons 2[M(CO)_nL_m]^{\cdot} \qquad (1)$$
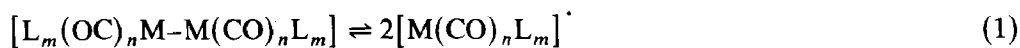
reactions are those of the metal-centred radicals, $[M(CO)_nL_m]^{\cdot}$ [1]. Of particular interest have been the reactions of such radicals which are believed to involve oxidative addition processes. Thus, complexes such as $[Co(CO)_3PBu^n_3]_2$ react with $SnHBu^n_3$ to yield $[Co(SnBu^n_3)(CO)_3PBu^n_3]$ and H_2 by a complex mechanism in which the two critical steps are as in eq. 2 and 3 [2]. It has also been suggested that

$$[M(CO)_nL_m]^{\cdot} \rightleftharpoons [M(CO)_{n-1}L_m]^{\cdot} + CO \qquad (2)$$

$$[M(CO)_{n-1}L_m]^{\cdot} + SnHBu_3 \rightarrow [M(H)SnBu_3(CO)_{n-1}L_m] \qquad (3)$$

---

* Author to whom correspondence should be addressed.

the reaction of $[Mn_2(CO)_8(PR_3)_2]$ (R = Bu, OEt) with HCl yielding $[MnH(CO)_4PR_3]$ and $[MnCl(CO)_4PR_3]$, a reaction which is a formal oxidative addition across a metal–metal bond, involves direct oxidative addition of HCl to the intermediate 15-electron radical, $[Mn(CO)_3PR_3]^{\bullet}$, to give $[Mn(H)Cl(CO)_3PR_3]$ as the crucial intermediate [3].

We have been interested in the reactions of dinuclear metal complexes with halocarbons [4] and have examined such reactions under photochemical conditions, with the aim of employing the oxidative addition reaction to produce halogeno and alkyl metal complexes. This aim has been realised in the case of complexes of the type $[Mn_2(CO)_8(PR_3)_2]$ and a preliminary account of this study has appeared [5]. We now present a complete report of this work, together with the results of additional experiments which allow considerable insight into the mechanism of reactions of this type.

Results and discussion

(i) Reactions of $[Mn_2(CO)_8(PBu_3)_2]$ * with alkyl halides

These photochemical reactions were all performed with a ten-fold excess of alkyl halide in degassed solvent under nitrogen, samples being periodically removed for analysis by infrared spectroscopy.

Reaction with benzyl chloride was clean, forming $[MnCH_2Ph(CO)_4PBu_3]$ and $[MnCl(CO)_3PBu_3]$ at approximately equal rates over a period of several hours (Fig. 1). The products were characterised by spectroscopic methods and by comparison with authentic samples ($[MnCH_2Ph(CO)_4PBu_3]$, infrared spectrum: 2050(m), 1988 (m), 1961 (s), 1938 (m) cm^{-1}; ^{1}H NMR spectrum: δ 1.0 (9H)t, CH$_3$; 1.2–1.5 (18H)m, CH$_2$(PBu$_3$); 2.0 (2H)d ($J(^{31}P–H) = 6$ Hz), CH$_2$(CH$_2$Ph); 7.1–7.6 δ(5H)m,
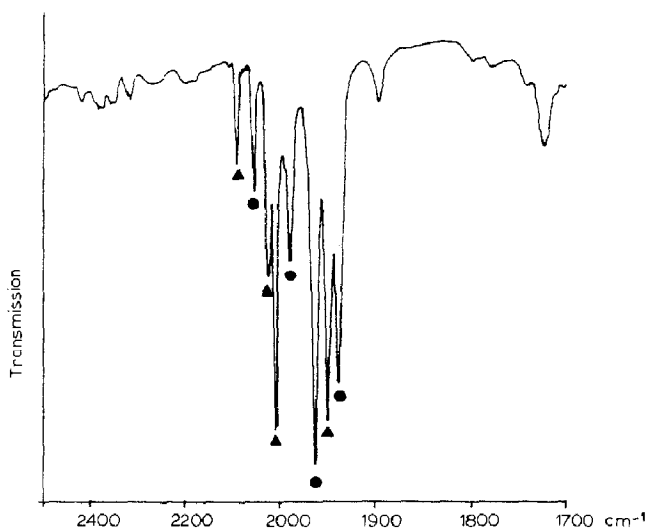
Fig. 1. Infrared spectrum of the reaction between $[Mn_2(CO)_8(PBu_3)_2]$ and PhCH$_2$Cl after 200 min ($\bullet$ = $[MnCH_2Ph(CO)_4PBu_3]$ peaks, $\blacktriangle$ = $[MnCl(CO)_4PBu_3]$ peaks).

---

* Throughout this paper PBu$_3$ refers to tri-n-butylphosphine.

C_6H_5. [MnCl(CO)PBu$_3$], infrared spectrum: 2087(w), 2028(m), 2010(s), 1950(s) cm^{-1}). There was no evidence for the generation of any other metal complexes in the early stages of the reaction and GC analysis of reaction mixtures did not indicate the formation of dibenzyl or toluene. After extended reaction periods, infrared spectra showed bands due to [MnCl(CO)$_3$(PBu$_3$)$_2$].

Reaction with PhCH$_2$Br appeared to give only [MnBr(CO)$_4$PBu$_3$]. However, when a solution of [MnCH$_2$Ph(CO)$_4$PBu$_3$] was photolysed in the presence of PhCH$_2$Br, it was converted into the bromo complex. Similar treatment of the benzyl complex with PhCH$_2$Cl did not lead to any reaction. Thus, it is possible that a common mechanism operates for both benzyl chloride and bromide.

Photolysis of PhCH$_2$CH$_2$Cl and [Mn$_2$(CO)$_8$(PBu$_3$)$_2$] resulted in only a slow reaction. After 17 h the infrared spectrum showed peaks due to [MnCl(CO)$_4$PBu$_3$] and a peak at 2050 cm^{-1} (hexane solution) tentatively assigned to [MnCH$_2$CH$_2$Ph-(CO)$_4$PBu$_3$]. Unfortunately, any other peaks arising from the alkyl complex in this reaction were obscured by the intense absorptions from residual dimer. The reaction involving PhCH$_2$CH$_2$Br proceeded smoothly over 3 h and both [MnBr(CO)$_4$PBu$_3$] and [Mn(CH$_2$CH$_2$Ph)(CO)$_4$PBu$_3$] (2050 (m), 1972 (m), 1959 (s), 1936 (s) cm^{-1}) were easily identified. Photolysis for a further 17 h led to disappearance of the peaks arising from the alkyl complex, while those from the bromo complex continued to grow in intensity.

In the case of MeI, there was evidence for a thermal reaction before photolysis commenced. After photolysis for 1 h, the infrared spectrum clearly showed the presence of both [MnI(CO)$_4$PBu$_3$] (2091(m), 2020(m), 1999(s), 1952(s) cm^{-1}) and [MnMe(CO)$_4$PBu$_3$] (2059(m), 1482(m), 1963(s), 1936(s) cm^{-1}), but it has not proved possible to exclude thermal activation completely in this case.

By comparison with the above reactions, those involving PhCl and PhBr were both exceedingly slow. Even after irradiation for 250 h, unchanged dimer predominated. In the former reaction, weak peaks were observed in the infrared spectrum which may be tentatively assigned to [MnCl(CO)$_4$PBu$_3$] and [MnPh-(CO)$_4$PBu$_3$]. In the case of PhBr, peaks due to [MnBr(CO)$_4$PBu$_3$], [MnBr(CO)$_3$-(PBu$_3$)$_2$] (1945(s) and 1897(m) cm^{-1}) and [MnPh(CO)$_4$PBu$_3$] (2060(m), 1993(m), 1980(m), 1956(s) cm^{-1}) were clearly visible.

(ii) Reactions of PhCH$_2$X (X = Cl, Br) with [Mn$_2$(CO)$_8$L$_2$] (L = CO, P(OMe)$_3$, P(OEt)$_3$, PEt$_3$, PPh$_3$)

Photolysis of [Mn$_2$(CO)$_{10}$] and PhCH$_2$X led to slow formation of [MnX(CO)$_5$], and [Mn(CH$_2$Ph)(CO)$_5$] (Fig. 2). The reaction of [Mn$_2$(CO)$_8$(PEt$_3$)$_2$] with PhCH$_2$Cl yielded both [MnCl(CO)$_4$PEt$_3$] (2095(m), 2028(m), 2010(s), 1950(m) cm^{-1}) and [MnCH$_2$Ph(CO)$_4$PEt$_3$] 2054(w), 1989(m), 1961(s), 1938(s) cm^{-1}). Similarly photolysis of [Mn$_2$(CO)$_8$\{P(OEt)$_3$\}$_2$] gave [MnCl(CO)$_4$P(OEt)$_3$] (2094(m), 2024(m) 2005(s), 1948(s) cm^{-1}) and [MnCH$_2$Ph(CO)$_3$P(OEt)$_3$] (2054 cm^{-1}). In this case the reaction was slow, and thus the other peaks arising from the benzyl complex were hidden under absorptions of the unreacted dimer. In the case of [Mn$_2$(CO)$_8$\{P(OMe)$_3$\}$_2$], the reaction was slower still, and even after 48 h only weak peaks at 2104 and 2070 cm^{-1} were observed in addition to those from the unchanged dimer. These were tentatively assigned to the chloro and benzyl complexes, respectively. The photolysis of [Mn$_2$(CO)$_8$(PPh$_3$)$_2$] and PhCH$_2$Cl was slower than any of the above reactions. Again, prolonged reaction resulted in only a
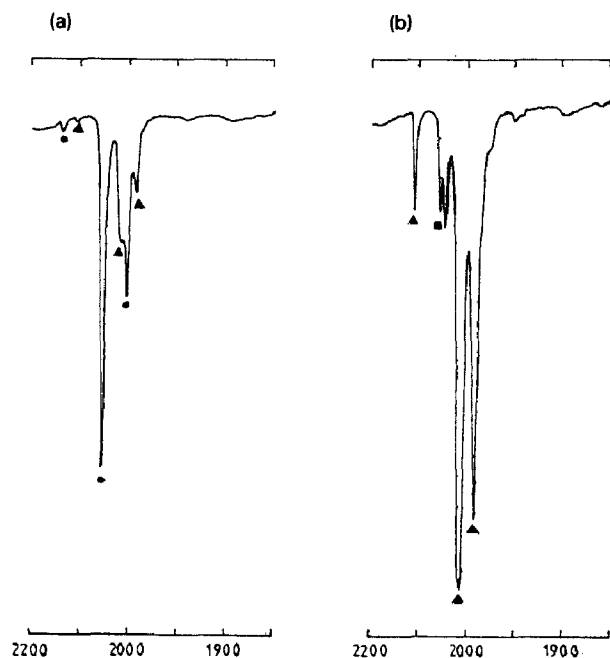
Fig. 2. Infrared spectra of the reaction products from (a) [Mn$_2$(CO)$_{10}$] and PhCH$_2$Br after 3 h ($\bullet$ = [MnBr(CO)$_5$] peaks, $\blacktriangle$ = [MnCH$_2$Ph(CO)$_5$] peaks) and (b) [Mn$_2$(CO)$_{10}$] and PhCH$_2$Cl after 30 h ($\blacksquare$ = [MnCl(CO)$_5$] peaks, $\blacktriangle$ = [MnCH$_2$Ph(CO)$_5$] peaks).

low conversion of the dimer, with tentative assignment of peaks at 2090 and 2052 cm^{-1} to the halo and benzyl complexes, respectively.
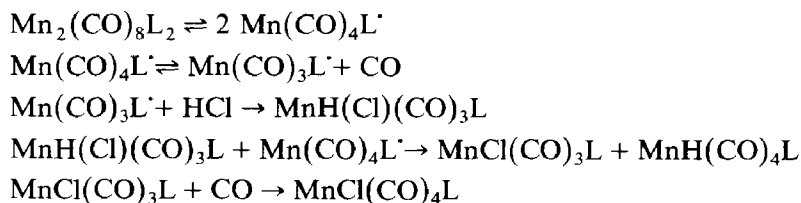
Reaction of the disubstituted dimers with PhCH$_2$Br gave [MnBr(CO)$_4$L] in all cases. Only in the case of the PPh$_3$ complex were additional weak peaks observed, suggesting the presence of the benzyl complex. However, in view of the finding that [MnCH$_2$Ph(CO)$_4$PBu$_3$] reacts with PhCH$_2$Br, it is likely that similar reactions occurred for these complexes.

(iii) Reactions of [Mn$_2$(CO)$_8$L$_2$] (L = CO, PBu$_3$, PEt$_3$) with PhCH$_2$Cl under CO

Photolysis of [Mn$_2$(CO)$_8$L$_2$] with PhCH$_2$Cl under a CO atmosphere led to a reduction in the rate of formation of the chloro and benzyl complexes (Fig. 3).

(iv) Kinetic and mechanistic study of the reaction of [Mn$_2$(CO)$_8$(PBu$_3$)$_2$] and PhCH$_2$Cl

Although the results described above parallel those for the reaction of [Mn$_2$(CO)$_8$(PR$_3$)$_2$] with HCl (Scheme 1), a number of alternative mechanisms are possible for such reactions. The mechanism proposed for the HCl reaction (Scheme 1) involves metal–metal bond homolysis followed by CO dissociation to generate a

$$Mn_2(CO)_8L_2 \rightleftharpoons 2\ Mn(CO)_4L^{\cdot}$$
$$Mn(CO)_4L^{\cdot} \rightleftharpoons Mn(CO)_3L^{\cdot} + CO$$
$$Mn(CO)_3L^{\cdot} + HCl \rightarrow MnH(Cl)(CO)_3L$$
$$MnH(Cl)(CO)_3L + Mn(CO)_4L^{\cdot} \rightarrow MnCl(CO)_3L + MnH(CO)_4L$$
$$MnCl(CO)_3L + CO \rightarrow MnCl(CO)_4L$$

Scheme 1
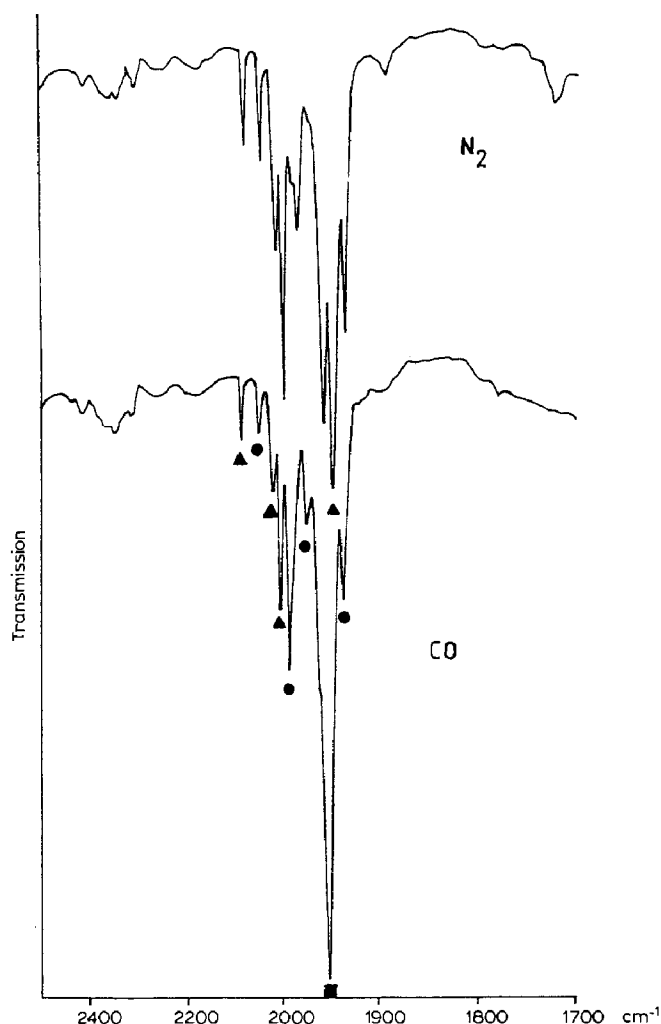
Fig. 3. Infrared spectra of the reaction between [Mn$_2$(CO)$_8$(PBu$_3$)$_2$] and PhCH$_2$Cl under N$_2$ and CO after 2 h ($\bullet$ = [MnCH$_2$Ph(CO)$_4$PBu$_3$] peaks, $\blacktriangle$ = [MnCl(CO)$_4$PBu$_3$] peaks, $\blacksquare$ = [Mn$_2$(CO)$_8$(PBu$_3$)$_2$] peaks).

reactive 15-electron intermediate, which subsequently undergoes oxidative addition of HCl. There is now overwhelming evidence that most reactions of 17-electron species with Lewis base two electron donors proceed via S_N2-type associative processes generating 19-electron intermediates rather than by dissociative processes involving 15-electron intermediates [1,6]. In the light of these findings, reactions which may involve oxidative addition, such as those of HCl and alkyl halides, must be reassessed.

Furthermore, the related reaction of [Rh(OEP)]$_2$ (OEP = octaethylporphyrin) with benzyl bromide has been shown to proceed by a radical chain process (Scheme 2, termination steps omitted) [7] and a similar mechanism may operate for reactions

$$[Rh(OEP)]_2 \rightleftharpoons 2[Rh(OEP)]^\cdot$$

$$[Rh(OEP)]^\cdot + PhCH_2Br \rightarrow [RhBr(OEP)] + PhCH_2^\cdot$$

$$PhCH_2^\cdot + [Rh(OEP)]_2 \rightarrow [Rh(CH_2Ph)(OEP)] + [Rh(OEP)]^\cdot$$
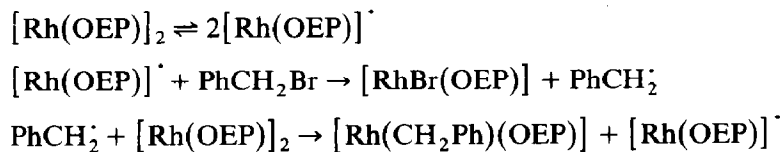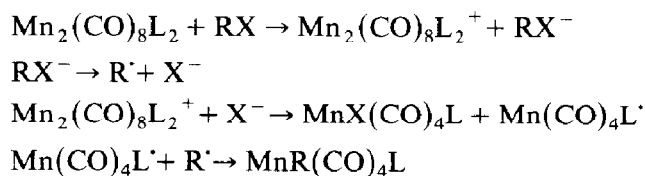
Scheme 2

of the manganese dimers. With these possibilities in mind, we considered that the mechanisms discussed below were worthy of consideration.
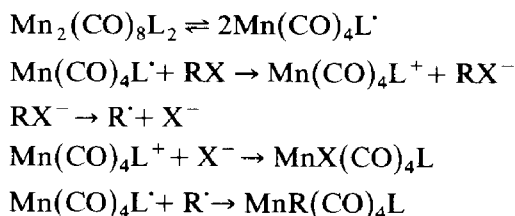
Firstly, a reaction paralleling that proposed for HCl may be operating. A steady-state treatment of such a reaction gives rise to the rate law shown in eq. 4.

$$\text{Rate} = \frac{k\left[\text{Mn}_2(\text{CO})_8\text{L}_2\right]^{1/2}[\text{RX}]}{k'[\text{CO}] + k''[\text{RX}]} \tag{4}$$
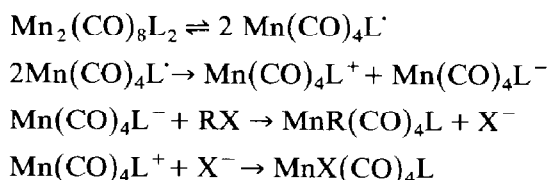
Some reactions of $[\text{Mo}_2(\text{CO})_6(\eta\text{-cp})_2]$ have been shown to follow an electron transfer pathway [8] and a similar reaction has been observed for photo-substitution of $[\text{Mn}_2(\text{CO})_{10}]$ by pyridine [9,10]. On the basis of these observations, three electron transfer reactions were considered in the present work. The first involves direct electron transfer from an excited state of the dimer (Scheme 3), the rate equation for

$\text{Mn}_2(\text{CO})_8\text{L}_2 + \text{RX} \rightarrow \text{Mn}_2(\text{CO})_8\text{L}_2{}^+ + \text{RX}^-$

$\text{RX}^- \rightarrow \text{R}^\cdot + \text{X}^-$

$\text{Mn}_2(\text{CO})_8\text{L}_2{}^+ + \text{X}^- \rightarrow \text{MnX}(\text{CO})_4\text{L} + \text{Mn}(\text{CO})_4\text{L}^\cdot$

$\text{Mn}(\text{CO})_4\text{L}^\cdot + \text{R}^\cdot \rightarrow \text{MnR}(\text{CO})_4\text{L}$

Scheme 3

$\text{Mn}_2(\text{CO})_8\text{L}_2 \rightleftharpoons 2\text{Mn}(\text{CO})_4\text{L}^\cdot$

$\text{Mn}(\text{CO})_4\text{L}^\cdot + \text{RX} \rightarrow \text{Mn}(\text{CO})_4\text{L}^+ + \text{RX}^-$

$\text{RX}^- \rightarrow \text{R}^\cdot + \text{X}^-$

$\text{Mn}(\text{CO})_4\text{L}^+ + \text{X}^- \rightarrow \text{MnX}(\text{CO})_4\text{L}$

$\text{Mn}(\text{CO})_4\text{L}^\cdot + \text{R}^\cdot \rightarrow \text{MnR}(\text{CO})_4\text{L}$

Scheme 4

$\text{Mn}_2(\text{CO})_8\text{L}_2 \rightleftharpoons 2\ \text{Mn}(\text{CO})_4\text{L}^\cdot$

$2\text{Mn}(\text{CO})_4\text{L}^\cdot \rightarrow \text{Mn}(\text{CO})_4\text{L}^+ + \text{Mn}(\text{CO})_4\text{L}^-$

$\text{Mn}(\text{CO})_4\text{L}^- + \text{RX} \rightarrow \text{MnR}(\text{CO})_4\text{L} + \text{X}^-$

$\text{Mn}(\text{CO})_4\text{L}^+ + \text{X}^- \rightarrow \text{MnX}(\text{CO})_4\text{L}$

Scheme 5

which is given in eq. 5. Alternatively, electron transfer may follow metal–metal bond homolysis (Scheme 4), giving the rate expression shown in eq. 6. Thirdly, electron transfer may be between two metal-centred radicals after metal–metal bond homolysis (Scheme 5, rate equation given by eq. 7).
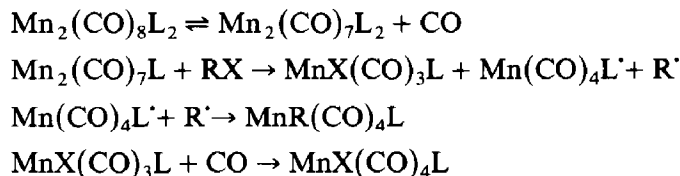
$$\text{Rate} = k\left[\text{Mn}_2(\text{CO})_8\text{L}_2\right][\text{RX}] \tag{5}$$

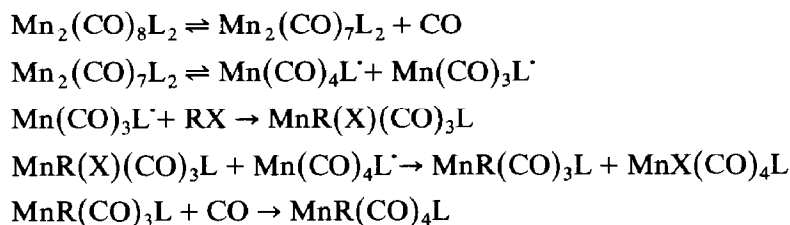$$\text{Rate} = k\left[\text{Mn}_2(\text{CO})_8\text{L}_2\right]^{1/2}[\text{RX}] \tag{6}$$

$$\text{Rate} = k\left[\text{Mn}_2(\text{CO})_8\text{L}_2\right] \tag{7}$$

Although much of the published work on the photochemistry of metal–metal bonded dimers involves homolytic fission leading to formation of metal-centred

radicals, the existence of processes involving the formation of coordinatively un-saturated dimers such as $[Mn_2(CO)_9]$ has been conclusively demonstrated in both thermal and photochemical reactions [11]. Two possible pathways involving such intermediates are considered here. Thus, initial ligand dissociation may be followed by direct attack of RX on the coordinatively unsaturated dimer (Scheme 6, eq. 8) or

$$Mn_2(CO)_8L_2 \rightleftharpoons Mn_2(CO)_7L_2 + CO$$

$$Mn_2(CO)_7L + RX \rightarrow MnX(CO)_3L + Mn(CO)_4L \cdot + R \cdot$$

$$Mn(CO)_4L \cdot + R \cdot \rightarrow MnR(CO)_4L$$

$$MnX(CO)_3L + CO \rightarrow MnX(CO)_4L$$

Scheme 6

$$Mn_2(CO)_8L_2 \rightleftharpoons Mn_2(CO)_7L_2 + CO$$

$$Mn_2(CO)_7L_2 \rightleftharpoons Mn(CO)_4L \cdot + Mn(CO)_3L \cdot$$

$$Mn(CO)_3L \cdot + RX \rightarrow MnR(X)(CO)_3L$$

$$MnR(X)(CO)_3L + Mn(CO)_4L \cdot \rightarrow MnR(CO)_3L + MnX(CO)_4L$$

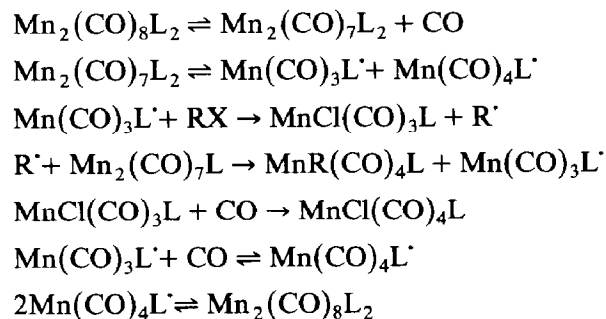$$MnR(CO)_3L + CO \rightarrow MnR(CO)_4L$$

Scheme 7

initial ligand dissociation may be followed by metal–metal bond homolysis and an oxidative addition reaction of RX to the 15-electron metal-centred radical. Scheme 7, eq. 9).

$$Rate = \frac{k[Mn_2(CO)_8L_2][RX]}{k'[CO] + k''[RX]} \tag{8}$$

$$Rate = \frac{k[Mn_2(CO)_8L_2]^{1/2}[RX]}{[CO]^{1/2}} \tag{9}$$

Finally, a mechanism which parallels that for $[Rh(OEP)]_2$ is shown in Scheme 8. This also gives a rate equation of the form given in eq. 9.

$$Mn_2(CO)_8L_2 \rightleftharpoons Mn_2(CO)_7L_2 + CO$$

$$Mn_2(CO)_7L_2 \rightleftharpoons Mn(CO)_3L \cdot + Mn(CO)_4L \cdot$$

$$Mn(CO)_3L \cdot + RX \rightarrow MnCl(CO)_3L + R \cdot$$

$$R \cdot + Mn_2(CO)_7L \rightarrow MnR(CO)_4L + Mn(CO)_3L \cdot$$

$$MnCl(CO)_3L + CO \rightarrow MnCl(CO)_4L$$

$$Mn(CO)_3L \cdot + CO \rightleftharpoons Mn(CO)_4L \cdot$$

$$2Mn(CO)_4L \cdot \rightleftharpoons Mn_2(CO)_8L_2$$

Scheme 8

Clearly, many of these possibilities can be distinguished by determination of the orders of reaction with respect to the metal complex and alkyl halide. These kinetic measurements were made using a merry-go-round photochemical reactor. The order
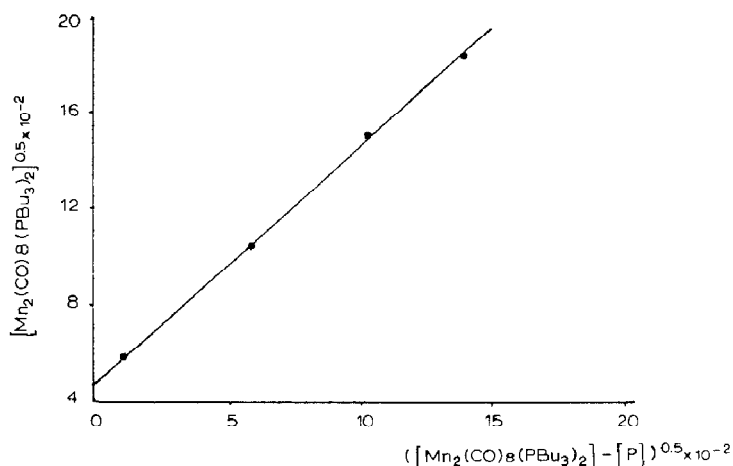
Fig. 4. Plot of kinetic data obtained using the half order relationship for $[Mn_2(CO)_8(PBu_3)_2]$ given in eq. 11.

with respect to metal dimer concentration was determined by the isolation method in which the concentration of benzyl chloride was maintained at a high value, so that its concentration could effectively be regarded as constant. All the kinetic reactions were performed in degassed hexane with a typical irradiation time of 3 h. The concentrations of products formed were determined by infrared spectroscopy by use of the band at 2087 cm^{-1} arising from the chloro complex and the band at 2050 cm^{-1} arising from the benzyl complex. The molar absorptivities of these bands were determined in the usual way with carefully purified samples. Because of the nature of these kinetic experiments, with several samples of different concentration being irradiated for the same time interval, time is a constant, and it was therefore necessary to use an integrated rate expression. All the above Schemes have either a first or half order dependence on metal complex concentration and the integrated rate expressions for these two orders are given in eq. 10 and 11, respectively ([P] = concentration of product).

$$\ln\left[Mn_2(CO)_8L_2\right] = \ln\left(\left[Mn_2(CO)_8L_2\right] - [P]\right) + Kt \tag{10}$$

$$\left[Mn_2(CO)_8L_2\right] = \left(\left[Mn_2(CO)_8L_2\right] - [P]\right)^{1/2} + Kt \tag{11}$$

A plot of typical data obtained by use of the 2050 cm^{-1} absorption of $[MnCH_2Ph(CO)_4PBu_3]$ for the half-order expression is shown in Fig. 4. This shows a slope of 0.99 and an intercept of 0.046 $M^{1/2}$. Two repeat determinations gave slopes and intercepts of 1.03 and 0.039 $M^{1/2}$ and 0.96 and 0.022 $M^{1/2}$ respectively. Data obtained by using the absorption of $[MnCl(CO)_4PBu_3]$ showed a deviation from these values with a slope of 0.82 and an intercept of 0.027 M (average of three determinations). The reason for this is that a significant amount of $[MnCl(CO)_3(PBu_3)_2]$ is formed by the end of the reaction, thereby reducing the validity of the later readings.

A plot of the data obtained using the absorption of the benzyl complex for the first order expression is given in Fig. 5. This shows a clear deviation from linearity. A best straight-line plot gives a slope of 0.69 (average of three determinations gives 0.68).
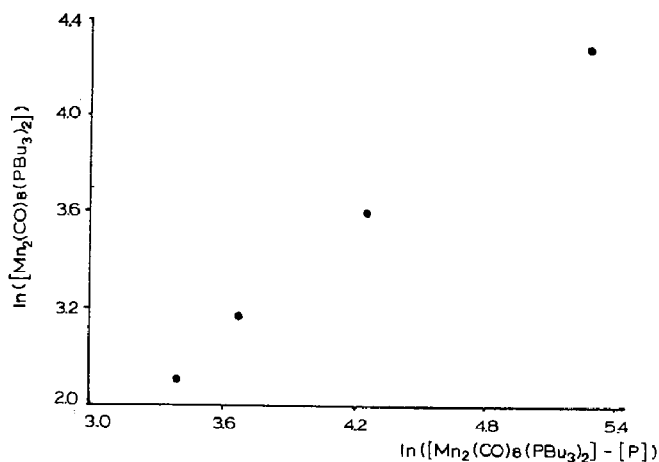
Fig. 5. Plot the kinetic data obtained using the first order relationship for $[Mn_2(CO)_8(PBu_3)_2]$ given in eq. 10.

The data are thus consistent with a half-order dependence on the concentration of the metal complex, and so the reaction cannot be proceeding by any of the mechanisms shown in Schemes 3, 5 and 6. Since the rate is lowered in the presence of CO, the mechanism shown in Scheme 4 may also be eliminated *.

Further definition of the reaction mechanism can be obtained from the determination of the order with respect to benzyl chloride. If a mechanism analogous to that shown in Scheme 1 obtains, then a dependence on benzyl chloride concentra-
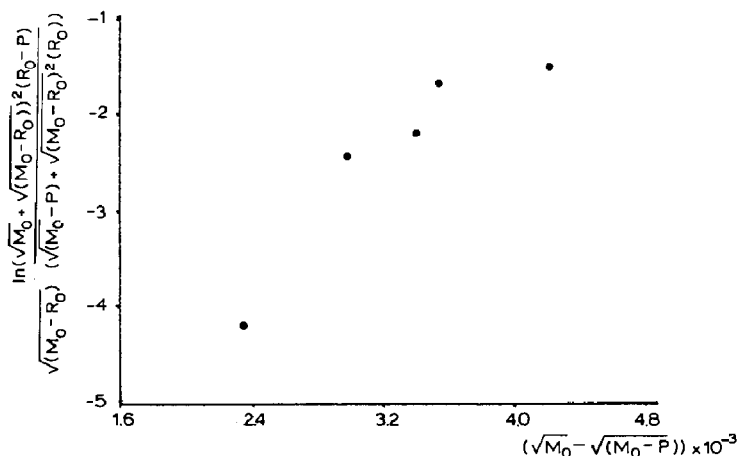
Fig. 6. Plot of the kinetic data obtained using the relationship shown in eq. 12 for a dependence of the type, $k[PhCH_2Cl]/1 + [PhCH_2Cl]$.

---

* Although Scheme 4 does not involve CO dissociation, it may be argued that, in the presence of CO, the intermediate $[Mn(CO)_4L]^+$ would undergo carbonylation to form $[Mn(CO)_5L]^+$, thereby reducing the rate of reaction with RX. Since the 18-electron cation is known to be stable, evidence for its formation might be expected in the infrared spectrum of the reaction mixture. No bands which might be assigned to $[Mn(CO)_5PBu_3]^+$ were observed.
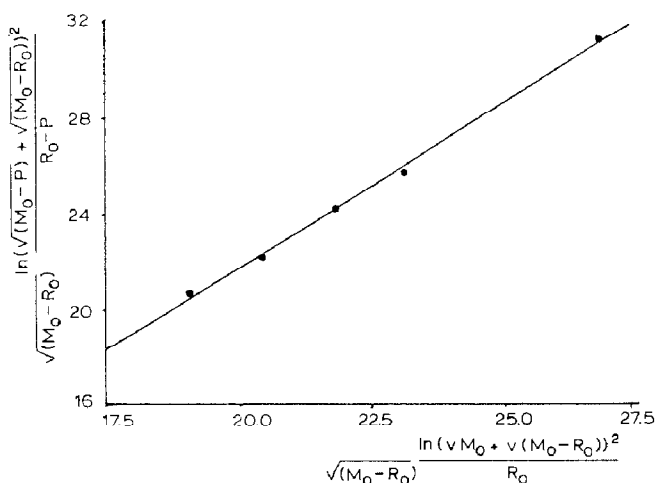
Fig. 7. Plot of the kinetic data obtained using the first order relationship for [PhCH$_2$Cl] given in eq. 13.

tion of the Michelis-Menton type (Rate $= k$[RX]$/1 +$ [RX]) would be expected, whereas the mechanisms shown in Schemes 7 and 8 have a first order dependence.

The determination of the order with respect to benzyl chloride was performed in a similar manner to that outlined above, but solubility limitations in the case of the metal dimer prevented use of the isolation method. Thus, the data had to be handled by use of the fully integrated rate expressions arising from eq. 4 and 9. These expressions are shown as equations 12 and 13, respectively. ($[M_0]$ and $[R_0]$ are the initial concentrations of metal dimer and alkyl halide respectively). Typical plots arising from use of eq. 12 and 13 are shown in Figs. 6 and 7, respectively. A linear relationship is only observed in Fig. 7, which suggests that the reaction follows either the mechanism shown in Scheme 7 or that given in Scheme 8.

$$\frac{k[CO]}{([M_0]-[R_0])^{1/2}} \cdot \ln \frac{\left\{[M_0]^{1/2}+([M_0]-[R_0])^{1/2}\right\}^2([R_0]-[P])}{\left\{([M_0]-[P])^{1/2}+([M_0]-[R_0])^{1/2}\right\}^2[R_0]}$$

$$= k^1 t + 2k \left\{[M_0]^{1/2}-([M_0]-[P])^{1/2}\right\} \quad (12)$$

$$\frac{1}{([M_0]-[R_0])^{1/2}} \cdot \ln \frac{\left\{([M_0]-[P])^{1/2}+([M_0]-[R_0])^{1/2}\right\}^2}{[R_0]-[P]}$$

$$= \frac{1}{([M_0]-[R_0])^{1/2}} \ln \frac{\left\{[M_0]^{1/2}-([M_0]-[R_0])^{1/2}\right\}^2}{[R_0]} + \frac{kt}{[CO]} \quad (13)$$

In an attempt to distinguish between these two possibilities we have studied the variation in quantum yield for the reaction between [Mn$_2$(CO)$_8$(PBu$_3$)$_2$] and PhCH$_2$Cl with change in concentration of the alkyl halide. Such an approach has been used previously to distinguish between chain and non-chain mechanisms for some related reactions. Thus, Kubiak et al. have shown that the quantum yield for photo-induced chlorine atom abstraction from CCl$_4$ by [M$_2$(CNMe)$_6$]$^{2+}$ (M$_2$ = Pt$_2$, Pd$_2$, PtPd) reaches a limiting value at low CCl$_4$ concentrations (5×10^{-3} to
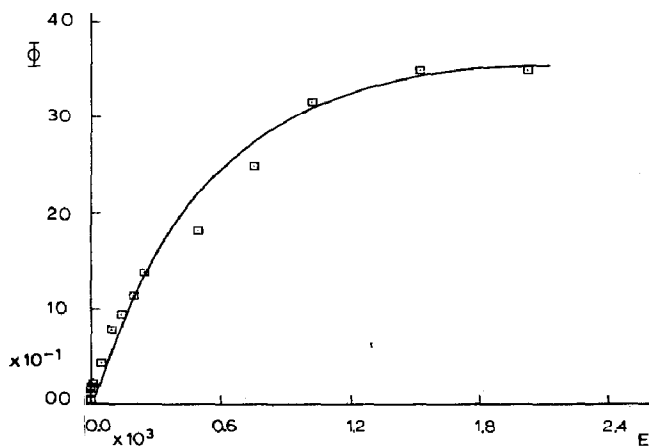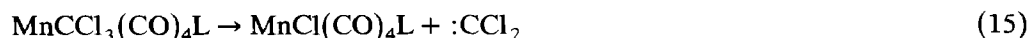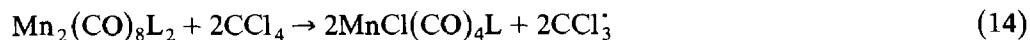
Fig. 8. Plot of the quantum yield versus the ratio $[PhCH_2Cl]/[Mn_2(CO)_8(PBu_3)_2]$ (E).

1×10^{-2} M depending on M_2, equivalent to a $[CCl_4]/[complex]$ ratio of ca. 100), which is consistent with a non-chain process [12]. In contrast, Pudephatt and co-workers have shown that photochemically initiated oxidative addition of 2-iodopropane to dimethyl (1,10-phenanthroline)platinum(II) shows a linear increase in quantum yield with haloalkane concentration up to 8×10^{-3} M (equivalent to a [haloalkane]/[complex] ratio of ca. 12.6) in agreement with the operation of a chain process [13]. A similar study of the variation in quantum yield with chloride ion concentration for the reaction with $[Mo_2(CO)_6(\eta\text{-cp})_2]$ shows a non-linear increase in quantum yield up to ca 0.2 M (equivalent to a $[Cl^-]/[complex]$ ratio of ca. 44), with a marked tail off above that value [14]. This was also interpreted in favour of a chain mechanism.

The data for the present reaction are shown in Fig. 8. The quantum yield (0.027 for a $[Mn_2(CO)_8(PBu_3)_2]/[PhCH_2Cl]$ ratio of 1/10 after irradiation for 3 h) increases in a non-linear fashion up to a $PhCH_2Cl$ concentration of ca 2 M, equivalent to a $[PhCH_2Cl]/[complex]$ ratio of about 1400–1500. In view of the very high alkyl halide concentration required to induce tail-off, we interpret this data in favour of a chain mechanism, and therefore suggest that the reaction follows the pathway given in Scheme 8.

It seems reasonable that this chain process, involving CO dissociation, might have a wider applicability than just to the reactions discussed above. It has previously been suggested that the reactions of dinuclear metal complexes with CCl_4 and other chlorocarbons proceed by simple atom abstraction processes (eq. 14) [15]. An alternative process is also possible, involving a mechanism of the type given in Scheme 8, which is followed by decomposition of the trichloromethyl complex by a route such as that shown in eq. 15. Such decomposition of $[CoCCl_3(CO)_4]$ and $[RhCCl_3(CO)L_2](L = thf$ or $PPh_3)$ has been proposed for reactions of CCl_4 with $[Co_2(CO)_8]$ and $[Rh_2(CO)_4L_4]$, respectively [16,17].

$$Mn_2(CO)_8L_2 + 2CCl_4 \rightarrow 2MnCl(CO)_4L + 2CCl_3^- \tag{14}$$

$$MnCCl_3(CO)_4L \rightarrow MnCl(CO)_4L + :CCl_2 \tag{15}$$

One possible test of the nature of the reaction between manganese dimers and CCl_4 involves performing such experiments under both nitrogen and carbon mono-
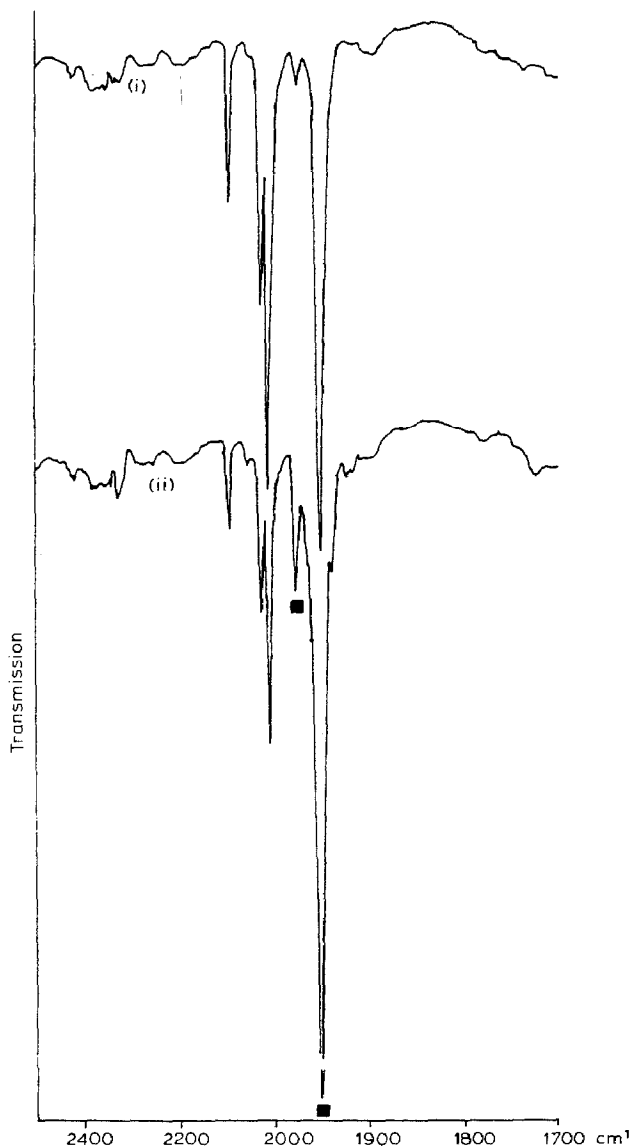
Fig. 9. Infrared spectra of the reaction between $[Mn_2(CO)_8(PBu_3)_2]$ and CCl_4 after 30 min under (i) N_2 and (ii) CO (■ = $Mn_2(CO)_8(PBu_3)_2]$ peaks).

xide. If the reactions are simple abstraction processes, the rate should be unaffected by the nature of the cover gas, whereas if a chain pathway analogous to Scheme 8 is being followed, rate retardation should be observed under CO. Figures 9 and 10 show a comparison of reactions performed under N_2 and CO involving CCl_4 and $[Mn_2(CO)_8(PBu_3)_2]$ and $[Mn_2(CO)_{10}]$, respectively. In both cases, significant retardation is observed under CO.

(v) Photochemical reactions of some dinuclear complexes of other metals with benzyl halides

In each case reactions with benzyl chloride and bromide were carried out under both N_2 and CO. The findings are summarised below.
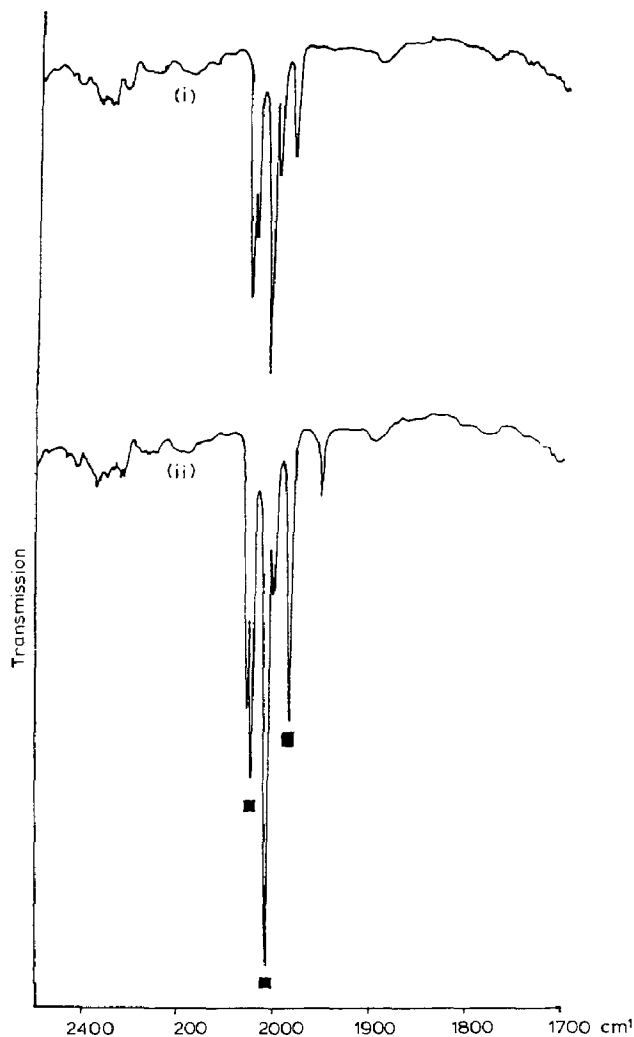
Fig. 10. Infrared spectra of the reaction between [Mn$_2$(CO)$_{10}$] and CCl$_4$ after 1 h under (i) N$_2$ and (ii) CO (■ = Mn$_2$(CO)$_{10}$ peaks).

(a) [Re$_2$(CO)$_{10}$]. Reaction with both benzyl chloride and bromide under N$_2$ gave rise to infrared absorptions of [ReX(CO)$_5$] only. The reactions were both retarded in the presence of CO and in the case of PhCH$_2$Cl, formation of [ReCH$_2$Ph(CO)$_5$] was also observed under CO. Presumably, the benzyl complex undergoes photochemical reactions with PhCH$_2$X which involve a CO dissociation step. This is sufficiently retarded in the case of reaction with PhCH$_2$Cl under CO to allow observation of the benzyl complex.

(b) [Mo$_2$(CO)$_6$(η-cp)$_2$]. Reactions with both benzyl halides under N$_2$ gave only [MoX(CO)$_3$(η-cp)], formation of the bromo complex being faster. Both reactions were slower in the presence of CO. [MoCH$_2$Ph(CO)$_3$(η-cp)] was found to be photochemically unstable in the presence of PhCH$_2$Cl and in this reaction [Mo(η^3-CH$_2$Ph)(CO)$_2$(η-cp)], [MoCl(CO)$_3$(η-cp)] and [Mo$_2$(CO)$_6$(η-cp)] were all formed prior to further reactions which yielded only the chloro complex as the final product.

(c) *[Fe₂(CO)₄(η-cp)₂]*. In this case only [FeX(CO)$_2$(η-cp)] (X = Cl, Br) is observed under both N$_2$ and CO. Both reactions were retarded under CO. Although [Fe(CH$_2$Ph)(CO)$_2$(η-cp)] reacts with benzyl bromide, the corresponding reaction with benzyl chloride is slow, suggesting that any benzyl complex formed in the reaction of the dimer should be observable by infrared spectroscopy. As this was not the case, the reaction of this dimer presumably has a different mechanism from that of the manganese complexes in its reaction with alkyl halides.

Experimental

All reactions were performed under dry deoxygenated nitrogen or, where appropriate, carbon monoxide. Solvents were purified by standard techniques and stored over sodium. All liquid phosphines and phosphites were vacuum distilled immediately prior to use. PPh$_3$ was recrystallised from ethanol. Alkyl halides were distilled from LiAlH$_4$ and stored under nitrogen.

Infrared spectra were recorded on a Perkin Elmer 782 spectrometer equipped with a 6300 data station. NMR spectra were recorded on a Bruker WP80 ft spectrometer. Kinetic and quantum yield measurements were made with a "merry-go-round" photochemical reactor, consisting of a rotating circular cell holder designed to hold up to 28 reaction tubes equidistant from a centrally placed Hanovia 500 watt medium pressure mercury lamp with slots for filters in the lamp support. This was placed in a thermostatted water bath maintained at 20°C stirred by the cell holder and contained in a light-tight cupboard. In the present study purple filters with absorption minima at 362 and 742 nm were placed around the lamp. This allowed transmittance of light of wavelength 366 nm which was used as the exciting wavelength. The samples being subjected to photolysis were contained in thick-walled pyrex tubes. The top half of each tube was wrapped in black PVC tape to prevent any stray light from reaching the samples. The tubes were capped with suba-seals, renewed for each reaction and through which they were degassed (by three flush-pump cycles), and samples were injected.

The complexes [Mn$_2$(CO)$_8$L$_2$] [18], [MnCl(CO)$_4$L] [19], [MnBr(CO)$_4$L] [20], [MnCH$_2$Ph(CO)$_4$L] [21], [Mo$_2$(CO)$_6$(η-cp)$_2$] [22], [MoCl(CO)$_3$(η-cp)] [23], [MoBr(CO)$_3$(η-cp)] [24], [MoCH$_2$Ph(CO)$_3$(η-cp)] [25], [Mo(η^3-CH$_2$Ph)(CO)$_2$(η-cp)] [26], [FeCl(CO)$_2$(η-cp)] [27], [FeBr(CO)$_2$(η-cp)] [28], and [Fe(CH$_2$Ph)(CO)$_2$(η-cp)] [29] were all prepared by literature methods. The molar absorbtivities of [MnCl(CO)$_4$PBu$_3$] and [MnCH$_2$Ph(CO)$_4$PBu$_3$] were determined by standard procedures and were found to be 995 M^{-1} cm^{-1} (2087 cm^{-1} band) and 1173 M^{-1} cm^{-1} (2050 cm^{-1} band), respectively.

Photochemical reactions of [Mn₂(CO)₈L₂] with alkyl halides

All the reactions were performed similarly. A weighed amount of the appropriate dimer (typically about 0.05 g) was placed in a small Schlenk tube, which was then degassed by several cycles of evacuation followed by flushing with nitrogen or carbon monoxide. An aliquot (10 cm^3) of degassed solvent was then syringed into the tube (the solvent was n-hexane in all cases, expect that of [Mn$_2$(CO)$_8$(PPh$_3$)$_2$], for which solubility limitations necessitated the use of benzene). After dissolution of the complex by gentle shaking, the alkyl halide was injected, a sample taken for

infrared analysis and photolysis started using a Hanovia 150 watt medium pressure mercury lamp. Samples were withdrawn periodically for infrared analysis. Irradiation was continued until the spectra showed no further change or, if the rate of change was slow, until the developing peaks were strong enough to allow identification.

In order to compensate for the strong infrared absorptions of benzene in the case of the [Mn$_2$(CO)$_8$(PPh$_3$)$_2$] reactions and strong absorptions of unreacted dimers in slow reactions (see Results and Discussion section), computer-aided peak subtraction routines were employed.

Photolysis of [MnCH$_2$Ph(CO)$_4$PBu$_3$] in the presence of PhCH$_2$Br

A solution of [MnCH$_2$Ph(CO)$_4$PBu$_3$] (0.035 g, 0.076 mmol) and PhCH$_2$Br (0.015 g, 0.067 mmol) in degassed hexane (10 cm^3) was placed in a Schlenk tube and irradiated for 12 h. Samples were removed for IR spectroscopic examination every 90 min, until complete conversion into the bromo complex was achieved.

Kinetic measurements

The method of preparation of solutions depended on the reaction parameter to be studied. In the case of the dependence on [Mn$_2$(CO)$_8$(PBu$_3$)$_2$] concentration, separate portions of the dimer were weighed into 10 cm^3 volumetric flasks, which were then stoppered with suba-seals. Typically, the samples ranged in weight from 0.05 to 0.25 g, giving concentrations of 7 to 27 mM. The flasks were then degassed through the septum cap using a long needle and kept under nitrogen.

In order to determine the order of reaction with respect to the dimer it was necessary to add an excess of PhCH$_2$Cl, and in order to ensure the same concentration of benzyl chloride in each of the solutions, 1 cm^3 of a stock solution of benzyl chloride (typically 3.6 g) in hexane (10 cm^3) was added to each of the volumetric flasks, which were then made up to the mark with degassed hexane. This provides a concentration of benzyl chloride of 280 mM in all solutions. Three aliquots of each solution were syringed into reactor tubes which were then loaded into the "merry-go-round" apparatus. The progress of the reactions were periodically monitored by infrared analysis of small samples of the solution of lowest dimer concentration. Irradiation was stopped when the peaks were of sufficient intensity to allow accurate absorbance measurements, which was, typically, after ca 3 h.

In determining the order with respect to benzyl chloride, a stock solution of [Mn$_2$(CO)$_8$(PBu$_3$)$_2$] (typically 1 g) in degassed hexane (50 cm^3) was prepared. This is a saturated solution ($\sim$ 27 mM) and so effectively limited the upper level of the range of benzyl chloride concentrations that can be used. Because of this limit, it was not possible to weigh out the small amounts of benzyl chloride required with the required accuracy. Thus, a stock solution was diluted to the appropriate concentrations and these were added to volumetric flasks. Appropriate amounts of the stock solution of the dimer were added and hexane added to the mark. These solutions were loaded into reactor tubes and irradiated for 24 h.

Determination of the lamp radiant flux

The lamp flux was determined by use of a solution of Aberchrome 540 in hexane (4.99 mM). Three aliquots (2 cm^3) were photolysed for 2 min on three occasions in between each set of photolysis reactions. The absorbance of each aliquot was

measured immediately, after being transported to the UV spectrometer in the dark to avoid conversion of Aberchrome 540 back to its unphotolysed form. The lamp radiant flux was calculated by the standard method using eq. 16. (I = radiant flux (photons s^{-1}), ΔA = change in absorbance, Φ = quantum yield (photon^{-1}), ϵ = molar absorbtivity, t = time of irradiation, l = path length, N = Avogadro's number) [30].

$$I = \frac{\Delta A.V.N}{\Phi.\epsilon.t.l} \qquad (16)$$

Determination of the quantum yield

[Mn$_2$(CO)$_8$(PBu$_3$)$_2$] (0.1845 g, 0.025 mmol) was weighed into a volumetric flask (25 cm^3), which was then degassed. Benzyl chloride (0.3 cm^3, 2.6 mmol) was introduced from syringe and hexane added to the mark. Aliquots of this solution were added to 4 reaction tubes which were placed in the "merry-go-round" reactor and irradiated for 20 h. The infrared spectrum of each solution was recorded and the quantum yield calculated using eq. 16. The value obtained for [Mn$_2$(CO)$_8$(PBu$_3$)$_2$] = 0.01 M, [PhCH$_2$Cl] = 0.1 M was 0.027 (average of three separate determinations each using 4 samples).

Determination of quantum yield with varying PhCH$_2$Cl concentration

[Mn$_2$(CO)$_8$(PBu$_3$)$_2$] was weighed into volumetric flasks and these were degassed as described above. For low concentrations of benzyl chloride (1, 2, 5, 7 and 10 equivalents), benzyl chloride was added from a stock solution. For higher concentrations (50, 100, 150, 200, 250, 500, 750, 1025, 1525, and 2025 equivalents), this reagent was added by syringe. Hexane was then added to the mark. Aliquots were transferred to reactor tubes (3 per concentration) and photolysed for 20, 3 or 1 h.

Table 1

Quantum yield measurements for photolysis of [Mn$_2$(CO)$_8$(PBu$_3$)$_2$] in the presence of various concentrations of PhCH$_2$Cl

[Mn$_2$(CO)$_8$(PBu$_3$)$_2$] (mM)	[PhCH$_2$Cl] (mM)	Ratio	Irradiation time (h)	Φ
0.10	0.10	1/1	20	0.004
0.10	0.20	1/2	20	0.006
0.10	0.50	1/5	20	0.016
0.10	0.70	1/7	20	0.019
0.10	1.00	1/10	20	0.022
0.05	2.50	1/50	3	0.044
0.05	5.00	1/100	3	0.079
0.05	7.50	1/150	3	0.094
0.05	10.00	1/200	3	0.114
0.05	12.50	1/250	3	0.138
0.04	20.00	1/500	1	0.183
0.04	30.00	1/750	1	0.250
0.04	41.00	1/1025	1	0.316
0.04	61.00	1/1525	1	0.350
0.04	81.00	1/2025	1	0.350

Concentrations of product were determined as described above. Solutions of benzyl chloride in hexane were photolysed in parallel with these solutions and infrared absorptions for these were computer-subtracted from those of the appropriate $[Mn_2(CO)_8(PR_3)_2]$/$PhCH_2Cl$ solutions. The results of these experiments are given in Table 1.

Acknowledgements

References

1 M.C. Baird, Chem. Rev., 88 (1988) 1217.
2 R.W. Wegman and T.L. Brown, Organometallics, 1 (1982) 47.
3 B.H. Byers, T.P. Curran, M.J. Thompson and L.J. Sauer, Organometallics, 2 (1983) 459.
4 R. Davis and I.F. Groves, J. Chem. Soc., Dalton Trans., (1982) 2281; W.J. Bland, R. Davis and J.L.A. Durrant, J. Organomet. Chem., 280 (1985) 95 and 397.
5 M.A. Biddulph, R. Davis, C.H.J. Wells and F.I.C. Wilson, J. Chem. Soc., Chem. Commun., (1985) 1287.
6 D. Astruc, Chem. Rev., 88 (1988) 1189.
7 R.S. Poonessa, N.C. Thomas and J. Halpern, J. Am. Chem. Soc., 107 (1985) 4333.
8 S. Amer, G. Kramer and A. Poe, J. Organomet. Chem., 209 (1981) C28.
9 A. Marcomi and A. Poe, J. Am. Chem. Soc., 105 (1983) 6952.
10 A. Poe and C. Sekhar, J. Chem. Soc., Chem. Commun., (1983) 566.
11 T. Kobayashi, H. Ohtani, H. Noda, S. Tertani, H. Yamazaki and K. Yasufuku, Organometallics, 5 (1986) 110.
12 M.K. Reinking, M.L. Kullberg, A.R. Cutler and C.P. Kubiak, J. Am. Chem. Soc., 107 (1985) 3517.
13 R.H. Hill and R.J. Puddephatt, J. Am. Chem. Soc., 107 (1985) 1218.
14 C.E. Philbin, C.A. Granatir and D.R. Tyler, Inorg. Chem., 25 (1986) 4806.
15 R.S. Herrick, T.R. Herrington, H.W. Walker and T.L. Brown, Organometallics, 4 (1985) 42.
16 B.L. Booth, R.N. Hazeldine and T. Inglis, J. Chem. Soc., Dalton Trans., (1975) 1851.
17 B.L. Booth, G.C. Casey and R.N. Hazeldine, J. Organomet. Chem., 224 (1982) 197.
18 J. Lewis, A.R. Manning and J.R. Miller, J. Chem. Soc. A, (1966) 845.
19 A.R. Manning, G. McNally, R. Davis and C.C. Rowland, J. Organomet. Chem., 259 (1983) C15.
20 P.W. Jolly and F.G.A. Stone, J. Chem. Soc. A, (1965) 5259.
21 R.B. King, Acc. Chem. Res., 3 (1970) 417.
22 R.B. King and F.G.A. Stone, Inorg. Synth., 7 (1963) 104.
23 M.S. Wrighton and D.S. Ginley, J. Am. Chem. Soc., 97 (1975) 4246.
24 J.W. Faller and A.S. Anderson, J. Am. Chem. Soc., 92 (1970) 5852.
25 R.B. King and A. Fronzaglia, J. Am. Chem. Soc., 88 (1966) 709.
26 T.Y. Luh and C.S. Wong, J. Organomet. Chem., 287 (1985) 231.
27 E.O. Fischer and E. Moser, Inorg. Synth., 12 (1968) 36.
28 B.F. Hallam and P.L. Pauson, J. Chem. Soc., (1956) 3030.
29 J.P. Bibler and A. Wojcicki, J. Am. Chem. Soc., 88 (1966) 4862.
30 H.G. Heller and J.R. Langan, J Chem. Soc., Perkin II, (1981) 341.